Neutron and photon out-of-field doses at cardiac implantable electronic device (CIED) depths

Hossein Aslian [a,b,*], Mara Severgnini [c], Navid Khaledi [d], Stefano Ren Kaiser [c], Anna Delana [e], Rossella Vidimari [c], Mario de Denaro [c], Francesco Longo [a,f]

[a] Department of Physics, University of Trieste, Trieste, Italy
[b] Department of Radiation Oncology, Olivia Newton-John Cancer Wellness & Research Centre, Austin Hospital, 145 Studley Road, Heidelberg, VIC, Australia
[c] Department of Medical Physics, Azienda Sanitaria Universitaria Integrata di Trieste, Trieste, Italy
[d] Department of Physics, Faculty of Science, Ryerson University, Toronto, ON, Canada
[e] Department of Medical Physics, S. Chiara Hospital, APSS, Trento, Italy
[f] Istituto Nazionale di Fisica Nucleare, Sezione di Trieste, Trieste, Italy

ARTICLE INFO

Keywords:
Out-of-field dose
Monaco
Monte Carlo
MCNPX
microDiamond
PinPoint 3D
Semiflex 3D
Cardiac implantable electronic devices
Secondary neutrons

ABSTRACT

The accuracy of an out-of-field dose from an Elekta Synergy accelerator calculated using the X-ray Voxel Monte Carlo (XVMC) dose algorithm in the Monaco treatment planning system (TPS) for both low-energy (6 MV) and high-energy (15 MV) photons at cardiac implantable electronic device (CIED) depths was investigated through a comparison between MCNPX simulated out-of-field doses and measured out-of-field doses using three high spatial and sensitive active detectors. In addition, total neutron equivalent dose and fluence at CIED depths of a 15-MV dose from an Elekta Synergy accelerator were calculated, and the corresponding CIED relative neutron damage was quantified. The results showed that for 6-MV photons, the XVMC dose algorithm in Monaco underestimated out-of-field doses in all off-axis distances (average errors: −17% at distances $X < 10$ cm from the field edge and −31% at distances between $10 < X \leq 16$ cm from the field edge), with an increasing magnitude of underestimation for high-energy (15 MV) photons (up to 11%). According to the results, an out-of-field photon dose at a shallower CIED depth of 1 cm was associated with greater statistical uncertainty in the dose estimate compared to a CIED depth of 2 cm and clinical depth of 10 cm. Our results showed that the relative neutron damage at a CIED depth range for 15 MV photon is 36% less than that reported for 18 MV photon in the literature.

1. Introduction

The ultimate goal of radiotherapy is not only to accurately deliver a very high dose to the target but also to reduce the nontarget dose to normal tissues. In-field nontarget doses are generally high, but they are precisely calculated and optimized by treatment planning systems (TPSs) (Kry et al., 2017). However, out-of-field nontarget doses are relatively small and cannot be accurately calculated by TPSs (Howell et al., 2010; Huang et al., 2013). This occurs because sources of out-of-field radiation, such as collimator scatter, head leakage, and patient scatter, are typically underestimated by TPSs (Kry et al, 2006, 2007).

Although the out-of-field dose may be sufficiently low compared with in-field dose, it can be a concern for pediatric patients and might increase the risk of secondary cancers, skin cancer, and cataract formation (Kry et al., 2017). Another group of patients in which out-of-field dose is of concern for is patients with cardiac implantable electronic devices (CIEDs). Such devices are susceptible to radiation damage, mainly caused by photoneutron produced in high energy radiotherapy, the cumulative dose effect, and transient oversensing as a result of the high dose rate (Aslian et al, 2019, 2020; Miften et al., 2019).

The CIEDs are usually placed in the left clavicular region at 0.5–2 cm below the patient's skin (Aslian et al., 2018). Patients undergoing thoracic radiotherapy will receive higher CIED dose than those treated in other regions. However, risk stratification based on CIED dose cannot be a sufficient estimator, as some studies reported devices malfunctioning after radiation exposure at doses lower than the historical threshold dose of 2 Gy, while other studies did not report CIED

* Corresponding author. Department of Physics, University of Trieste, Via Alfonso Valerio, 2, 34127, Trieste, Italy.
E-mail addresses: hossein.aslian@phd.units.it, h-aslian@mail.com (H. Aslian).

dysfunctions even at CIED doses higher than 50 Gy (Aslian et al., 2020; Gauter-Fleckenstein et al., 2020).

In new AAPM practice guidelines to manage CIED patients receiving radiotherapy (TG-203) (Miften et al., 2019), CIED patients are risk categorized not only on the basis of the CIED cumulative dose and pacing dependency but also on the basis of neutrons present. TG-203 also discussed several related challenges to each potential risk, including accurate estimation of CIED dose, out-of-field dose at CIED depth, and neutron contamination. For example, it is recommended that CIED dose estimation should be recorded based on either TPS calculation (if the CIED is within 3 cm of the treatment field edge) or in-vivo dosimetry (if distance from CIED to treatment field is between 3 and 10 cm).

Given that fast Monte Carlo (MC) algorithms are considered to be the most reliable and accurate method of dose calculation in radiotherapy, different vendors have developed fast MC-based TPS (Richmond et al., 2020; Snyder et al., 2019). Monaco, offered by Elekta (Elekta AB, Stockholm, Sweden), is one of the first commercial fast MC-based treatment planning systems. Currently, there are two fast MC-based dose calculation algorithms within Monaco, namely, X-ray voxelized Monte Carlo (XVMC) and graphical processing unit Monte Carlo (GPUMCD) (Clements et al., 2018). The XVMC originated from a virtual source model based on a study by Sikora et al. that considers different contributions (Sikora et al., 2007), such as primary photon source, secondary photon source and electron contamination (Gholampourkashi et al., 2019).

The general-purpose MC codes are built according to a microscopic approach which allows simulation of interactions and transport of particles with matter, starting from the fundamental properties of the atomic nucleus and of its constituents (Muraro et al., 2020). However, the fast MC-techniques used in TPS model the transport of radiation in the voxel medium with its associated cross sections and on a macroscopic level, which result in a faster computation time compared to the general-purpose MC codes. Some of the differences between the general-purpose MC codes and the MC-based TPS algorithms are discussed in detail by Jabbari (Jabbari, 2011).

Many studies have been conducted to evaluate the accuracy of out-of-field dose calculations in different photon-beam TPSs (e.g., Eclipse and Pinnacle) through different MC radiation transport codes (e.g., MCNP, Geant4, EGGnrc) (Huang et al., 2013; Kry et al, 2006, 2007; Puchalska and Sihver, 2015; Wang and Ding, 2014) or dosimetry measurements (Delana et al., 2020). A new study by Sánchez-Nieto et al. (2020) was published as one of the first studies focusing on the accuracy of the out-of-field dose calculations in Monaco. The study simulated the head of Elekta Axesse linac using the MC code EGSnrc and only for non-neutron-producing radiation (6 MV photon) and a 10 $\times$ 10 cm^2 square field at a depth of 5 cm.

Neutron contamination caused by high linear energy transfer (LET) radiation (high energy photon >10 MV or proton therapy) has deleterious effects on the memory or microprocessor circuits of CIEDs. The possibility of neutron-induced damage increases with increasing photon energy and subsequently higher neutron fluences. For example, the neutron flux at 18 MV is approximately 2 times and 10 times greater than the flux at 15 MV and 10 MV, respectively (Miften et al., 2019). Several studies investigated the mechanisms and sources of CIED malfunctions during radiotherapy with neutron-producing photon energies (E $\geq$ 10 MV). (Aslian et al., 2020; Koivunoro et al., 2011; Matsubara et al., 2020; Miften et al., 2019). Ezzati and Studenski (Ezzati and Studenski, 2017, 2019) proposed a method to quantify the relative neutron damage induced in CIEDs as a function of field size, off-axis distance and depth. They reported neutron damage induced in CIEDs of an 18 MV photon beam from Varian 2100C/D linac.

In this study, a detailed MC model of the Elekta Synergy linear accelerator head was first simulated to assess out-of-field doses from both low- (6 MV) and high-energy (15 MV) photons in a water phantom using MCNPX code. Then, the photon out-of-field doses obtained from Monaco calculations, measurements with three high spatial and sensitive detectors (microDiamond, PinPoint 3D, and Semiflex 3D ionization chamber) and the MC model at CIED depths of 1 and 2 cm were compared. Finally, the neutron equivalent dose and fluence at CIED depths were calculated using MCNPX, and the CIED relative neutron damage of a 15-MV photon beam from Elekta Synergy was quantified using the method suggested by Ezzati and Studenski (Ezzati and Studenski, 2017, 2019).

2. Methods and materials

2.1. Monte Carlo model

The Monte Carlo N-particle extended code (MCNPX, version 2.7, Los Alamos National Laboratory, Los Alamos, NM) (Pelowitz et al., 2011) was used to calculate the photon and neutron out-of-field doses in this study.

First, the head of an Elekta Synergy medical linear accelerator was modeled based on the manufacturer's detailed information and available data in the literature (Becker, 2007; Khaledi et al., 2018; Martnez Ovalle, 2013). With the development of software tools compatible with 3D computer-aided design (CAD) standard ACIS text (SAT) format, the complex geometry drawn by a CAD software can be converted or directly modeled into MCNP. In this simulation, the geometry of components and a 50 x 50 x 50 cm^3 MP3 water phantom were first drawn using AutoCAD software in SAT format. The MCNP visual editor (MCNPXVised, version 2.6) was used to covert the SAT file into an MCNP input file (Khaledi et al., 2018). Material compositions and the density of each specific component were defined in the data card section as indicated in the manufacturer's document. To define materials for shielding the head, available data in the literature were used given that the materials used by manufacturers to make head shielding are typically similar (Becker, 2007; Khaledi et al., 2018; Martnez Ovalle, 2013). The main materials and compositions are as follow: Target: tungsten (90%) and rubidium; target block: Cu (99.95%); primary collimator: tungsten (95%); primary scatter filter: Iron (68.5%), chromium, nickel and others; secondary flattening filter: mild steel (Fe: 99%); backscatter plate: aluminum alloy (Al: 98%); ceramic ion chamber: aluminum alloy (Al_2O_3: 96%); leaf: tungsten (95%); diaphragm: tungsten (95%); bending magnet: steel and copper with an outer tungsten and lead shielding, treatment head shielding: lead with an outer steel.

In the source definition section, the Gaussian energy spectrum and the spot size of the electron beam striking the target were initially selected based on the estimated values provided in the ELEKTA MC document. However, to obtain a percentage dose deviation of less than 3% between the measured and calculated practical range (Rp) and the depth of 50% maximum dose (R_{50}) in percentage depth dose (PDD) curves, these values were changed. The peak energy of 6.3 MeV and a FWHM of 0.5 MeV were selected for 6 MV X-ray beam energy; the values were 13.5 and 0.4 MeV for 15 MV X-ray beam energy.

The photon percentage depth dose curves, photon beam profiles and out-of-field doses were calculated at three depths, including 1 cm and 2 cm (approximate depths of CIED) (Aslian et al., 2018; Miften et al., 2019) as well as 10 cm (TRS-398 recommend clinical depth) ("Implementation of the International Code of Practice on Dosimetry in Radiotherapy (TRS 398): Review of Testing Results | IAEA"). Simulations were performed at a source-to-surface distance (SSD) of 100 cm for field sizes of 10 cm x 10 cm and 5 cm x 5 cm for 6 MV and 15 MV. The gantry was set to 0. The central axis of the beam in the water phantom were divided into 0.2 x 0.2 x 0.2 cm^3 voxels. The energy deposition from all types of particles in each voxel was scored using mesh tally type 3 and rmesh card which specifies a rectangular mesh. The average energy deposition per unit volume (MeV/cm^3 per source particle) were normalized to the deposited energy at the depth of the maximum dose (D_{max}). The relatively larger voxel sizes to score the energy deposition in out-of-field doses (compared with in-field) were defined to achieve

acceptable uncertainty levels (Kry et al, 2006, 2007). The voxel sizes were 1.0 x 0.2 x 0.2 cm^3 in the in-plane tallies and 0.2 x 1.0 x 0.2 cm^3 in the cross-plane tallies. These values were compared against the corresponding measurements. Note that the percentage difference between measured and simulated doses was estimated as a function of distance from the central axis using the following formula:

$$\text{Percentage difference} = \frac{(\text{Monte Carlo dose} - \text{Measured dose})}{(\text{Measured dose})} \times 100 \quad (1)$$

The neutron fluences from a Synergy accelerator operating at 15 MV were calculated using a tally (F5:n). Neutron fluxes were converted to ambient dose equivalent using conversion coefficients of ICRP 74 available in MCNPX (ICRP, 1996).

To reduce the statistical uncertainty and increase the computing efficiency, different variance reduction techniques were used (Khaledi et al, 2013, 2017). Energy cut-off (CUT card) was used from the specific truncation methods available in MCNPX. The applied electron and photon cutoff energies were 10 keV and 0.03 MeV, respectively. Geometry splitting from population control methods available in MCNPX was used, and importance values (IMP card) were assigned to each cell. From the modified sampling methods, bremsstrahlung production was biased on target materials for a 15-MV photon. The maximum number of particle histories was $5x10^8$ for 5 cm x 5 cm and $4x10^8$ for 10 cm x 10 cm. Photo-atomic and cross-section data were derived from MCPLIB04 and ENDF/B-VI.8 data library (Khaledi et al, 2013, 2017, 2018).

2.2. Irradiation and measurements

Irradiation was delivered using an Elekta Synergy linac at the University hospital of Trieste, Italy. The photon dosimetric measurements were performed in a large-size MP3 water tank with a scanning range of 600 x 500 x 408 mm^3 (PTW-Freiburg, Germany). The system was operated using MEPHYSTO mc^2 software and TBA electronics. The dosimeters were connected to a PTW UNIDOS E universal dosimeter for response measurements and a Tandem Dual-channel electrometer for scanning measurements (PTW-Freiburg, Germany).

First, the accuracies of the MC models for both 6 MV and 15 MV were verified at the central beam axis and in the photon out-of-field measurements, as recommended by AAPM TG-158 (Kry et al., 2017). The percentage doses and beam profiles at D_{max}, at less than D_{max}, and at the reference depth for photon calibration (10 cm) were measured and compared against calculations. Here, measurements were made with a PTW Farmer ionization chamber (30013, sensitive volume of 0.6 cm^3). It should be noted that measurements were only performed for photon contribution, while neutron contribution was only estimated by MCNPX code.

The photon out-of-field dose profiles were measured using three different PTW (Freiburg, Germany) detectors, including a semiconductor and two air-filled ionization chambers up to an off-axis distance of 30 cm. First, a microDiamond detector (60003, sensitive volume of 0.004 mm^3), which is a synthetic single-crystal detector with an almost water equivalent for all beam energies and high sensitivity, was used. The second detector was a PinPoint 3D ionization chamber (31022, sensitive volume of 0.016 cm^3), and the third was a Semiflex 3D ionization chamber (31021, sensitive volume of 0.07 cm^3). All three selected detectors have a high spatial resolution and are suitable for standard (10 cm x 10 cm) and smaller field sizes. These detectors were almost new and were factory calibrated five months prior to the measurements. The detectors were precisely positioned based on the central axis and the detector's sensitive volume in a motorized water phantom. The high-precision stepper motors allow high positioning accuracy (±0.1 mm). Thus, step sizes of 3 mm in-field and 1 mm out-of-field were adjusted. The measurements were repeated at least three times to define the random errors and the positioning errors of the detector. Notably, all the measurements were implemented using the same geometric setup (gantry and collimator angle, SSD, field sizes and depth) that was used in the simulations. Similar to the MC calculations, out-of-field doses at both CIED depths and clinical depth were measured to better interpret the results.

2.3. Treatment planning system

The commercial Monaco TPS V.5.11.01 (Elekta AB, Stockholm, Sweden) with the X-ray voxel Monte Carlo (XVMC) dose calculation algorithm was used for photon dose calculations. A water phantom with the same size and setup was simulated in the TPS. In-field and out-of-field dose distributions for the above-mentioned field sizes, energies and depths up to an off-axis distance of 30 cm were calculated using the TPS in QA mode. Finally, the dose profiles were exported using the dose export tool for comparison with those obtained from measurements and MCNPX. The calculations were computed using a 0.2 × 0.2 × 0.2 cm^3 dose grid, a dose uncertainty of 0.5% and a beam statistical uncertainty of 1.0% per calculation for out-of-field doses. The results for 6 MV were compared with that of the recent published study (Sánchez-Nieto et al., 2020Sánchez-Nieto et al., 2020).

2.4. CIED relative neutron damage

In the testing and design of radiation-hardened electronics, the specific material of interest is silicon, and neutron fluence requirements are quoted in terms of a 1-MeV equivalent silicon damage (DePriest, 2014; Ezzati and Studenski, 2017). These features are chosen because the 1-MeV equivalent silicon damage function represents the most important metric in assessing neutron damage to semiconductors (DePriest, 2014). The updated E722 standard, which is an official document published by the American Standard for Testing Materials (ASTM) committee E10, attempted to derive the Norgett-Robinson-Torrens (NRT) damage energy factors that are used to define the 1-MeV(Si) equivalent fluence radiation damage metric. This document also provides MCNP users with free-field radiation response functions for the 1-MeV(Si) equivalent fluence to quantify radiation damage. The damage function represents the number of defects introduced by the incident neutrons, which is related to the number of displaced atoms in silicon lattice. Ezzati and Studenski (Ezzati and Studenski, 2017, 2019) used this function and specified the function to calculate relative CIED damage rather than an absolute damage metric. These researchers suggested parametrizing CIED damage as a function of field size, off-axis distance and depth by normalizing to damage on the beam central axis at the surface of the phantom:

$$\text{CIED relative damage} = \frac{CIED\ damage_{x,y,z}}{CIED\ damage_{0,0,0}} \quad (2)$$

The damage in this method is defined in Equation (2), where $\phi(E)$ is neutron fluence, and $DF(E)$ is neutron energy damage factor.

$$\text{Damage} = \int_{E_{min}}^{E_{max}} \phi(E) DF(E) dE \quad (3)$$

3. Results and discussion

3.1. Monte Carlo validation

In this study, an MC model of an ELEKTA-Synergy accelerator head operated at 6 and 15 MV was simulated to investigate the out-of-field doses from the photon.

Fig. 1 illustrates some parts of our MC simulation, but the detailed information cannot be shared publicly due to company policy and our nondisclosure agreement.

To validate our MC model, the calculated dose profiles as well as the

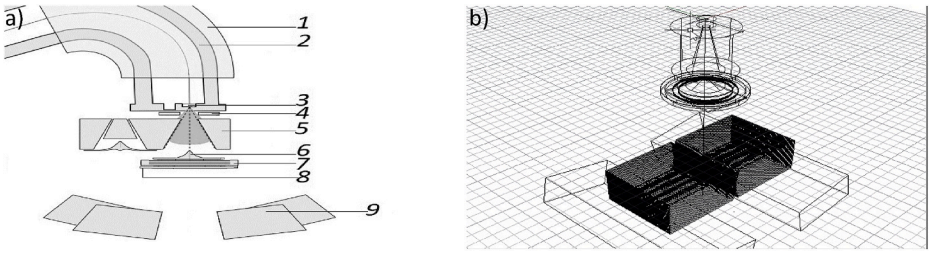

Fig. 1. (a) Scheme of the treatment head, including bending magnets (1), flight tube (2), target (3), primary scatter filter (4), primary collimator (5), secondary flattening filter (6), ceramic ion chamber (7), backscatter plate (8), and diaphragm (jaw) (9); 3D model of (b) some of the components of the linac such as target, primary collimator, secondary flattening filter, backscatter plate, ceramic ion chamber, MLCs and jaw.

PDDs for both energies and field sizes were compared with the corresponding measurements. The results are shown in Fig. 2. These two figures were followed by their point-by-point relative dose differences, which are shown in Fig. 3. In beam profiles, the differences in off-axis points within 50–100% isodose ranged between 0.5% and 1.4%, those in penumbra regions were between 2% and 3%, and those for the outside beam edge up to 20 cm were as high as 27.8%. In PDDs and buildup regions, the differences were between 2% and 10.3%, and the discrepancy ranged from 1% to 6% for data points on the central beam axis beyond the depth of D_{max}.

Venselaar et al. (2001) suggested a set of tolerances to evaluate dose calculation models. The recommended values of the tolerances for homogenous and simple geometry in the umbra, penumbra and build-up regions of the central beam axis and the outside beam edges are 2%, 10%, and 30%, respectively. Our results were within the accepted criteria but slightly higher for the buildup region. According to Mesbahi (2006), this finding might be due to the less accurate measurement of the ion chamber in the buildup region.

It should be noted that calculated and measured out-of-field dose profiles in both the in-plane and cross-plane directions were performed. Although they were not identical, their differences were small enough to be negligible (less than 2%).

Additionally, note that based on the MCNPX self-assessment tests for each tally, all 10 MCNP statistical checks were passed and most of the mesh cells have statistical errors below 5%.

3.2. *Out-of-field photon*

The left sides of Figs. 4 and 5 depict the comparisons between relative out-of-field doses in the cross-plane direction obtained from TPS-calculated, MC-simulated, and measurements for aforementioned depths, field sizes, and energies up to an off-axis distance of 30 cm.

According to the results, larger field size and higher beam energy lead to an increase of the out-of-field dose. This notion is well documented in the literature and is not the focus of this study (Kaderka et al., 2012; Kry et al., 2017; Puchalska and Sihver, 2015).

Good agreement between measured and simulated out-of-field doses was observed for both depths, energies, and field sizes, and the average difference was in the range of 3–20%.

Acceptable agreement was noted between the out-of-field doses measured by all three dosimeters at both depths, and the average differences between the results did not exceed 15% (min: 3.2%, max: 14.3%). Among those, PinPoint 3D almost always measured the highest. In contrast, the Diamond offered the lowest measurement, but the result was closer to that of the MC-simulated out-of-field doses.

Abdelaal et al. (2017) investigated the out-of-field does from a

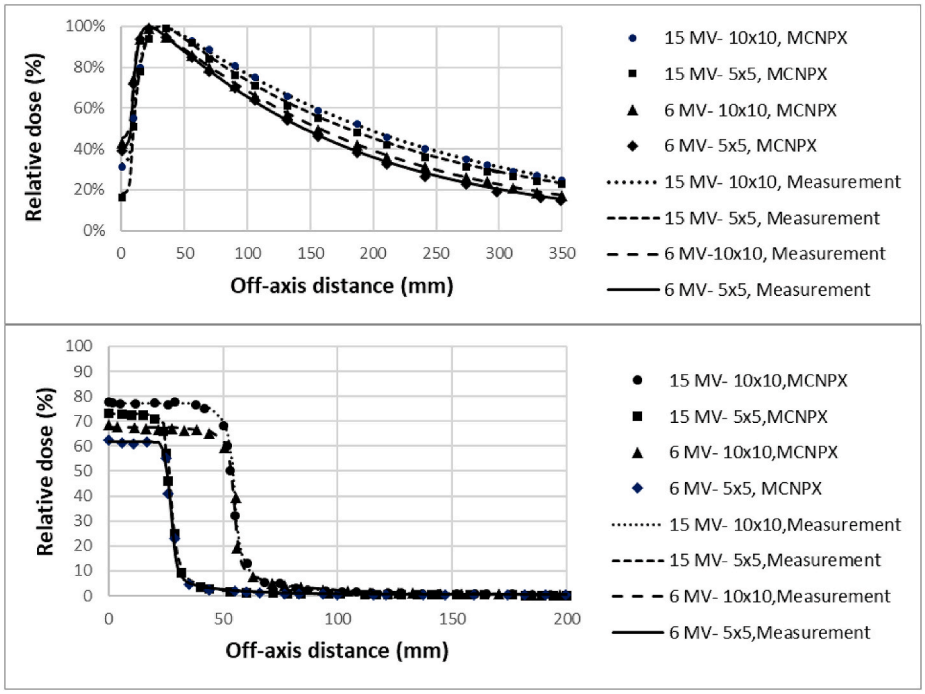

Fig. 2. (a) Comparison of MC-calculated and measured cross-plane beam profiles for field sizes of 10 cm x 10 cm and 5 cm x 5 cm for 6 MV and 15 MV at 10 cm depth. (b) MC calculated and measured PDD curves for aforementioned field sizes and energies.

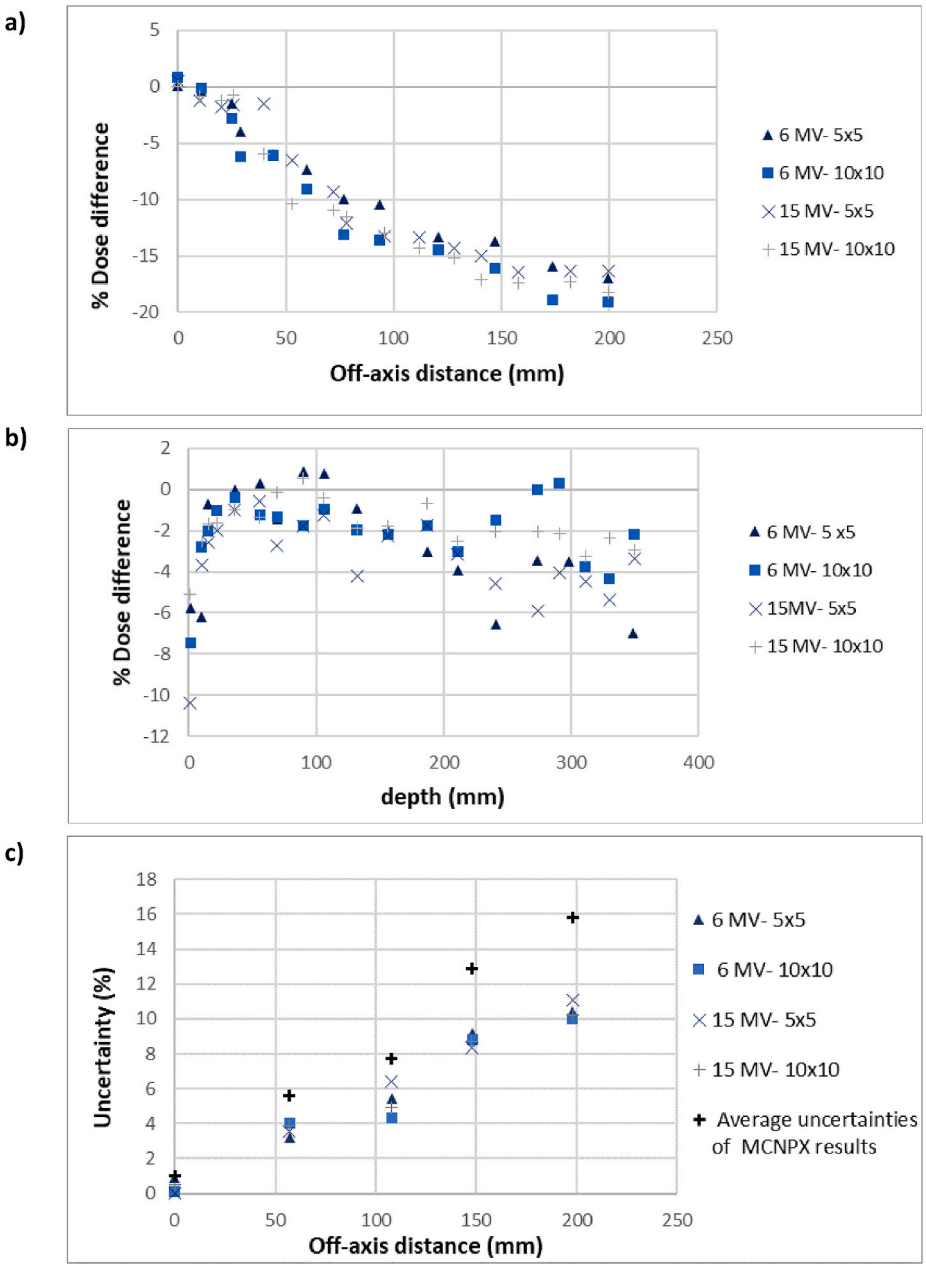

Fig. 3. Percent difference between simulated and measured **(a)** cross-plane beam profiles and **(b)** PDDs for data presented in Fig. 2. **(c)** The average uncertainty in the measured data ranged from 1% up to 11% and uncertainty associated with simulated data varied between 1.5% and 16%.

Siemens ONCOR linac using Semiflex (PTW, 31010) and PinPoint (PTW, 31014). Their results showed higher mean out-of-field doses measured with PinPoint compared to Semiflex for all field sizes, energies and depths. In this study, we used PinPoint 3D and Semiflex 3D, which are optimized versions of their predecessors. When comparing PinPoint with Semiflex, PinPoint 3D has a smaller sensitive volume and a higher sensitivity (Abdelaal et al., 2017) and response to low-energy Compton scatter (Martens et al., 2000) than Semiflex 3D.

The right sides of Figs. 4 and 5 show the average percentage differences between the results and the degrees to which the XVMC underestimated the actual measured doses in some off-axis points. In all the peripheral dose profiles calculated by using the XVMC, a sharp drop off was noted at an off-axis distance between 19 and 22 cm. In other words, the XVMC exhibited a severe underestimation of dose in areas greater than approximately 20 cm from the field edge.

As shown in these figures, XVMC reported a negligible dose (in the order of 0.01 cGy) for the off-axis points beyond 25 cm from the field edge. To verify that these results are reliable and comparable, we queried another center using the same version of the Monaco and linac to repeat the same calculations. According to their results, similar fall-off behaviors were noted for off-axis distances of 18–20 cm, and a negligible dose (<0.01 cGy) over distances greater than 25 cm from the field edge was calculated.

Fig. 6 showed a small dependency of the out-of-field photon doses on depth. However, the out-of-field photon doses increased with the increase in beam energy from 6 MV to 15 MV.

Some MC studies simulated out-of-field doses from low- and high-energy photons, most of which focused on Varian linac models (Bednarz and Xu, 2009; Cravo Sá et al., 2020; Kry et al, 2006, 2007). Kry et al. (Kry et al, 2006, 2007), and Bednarz and Xu (2009) simulated the head of Varian Clinac using MCNPX to investigate out-of-field doses from low- (6 MV) and high-energy (18 MV) photons. The design and

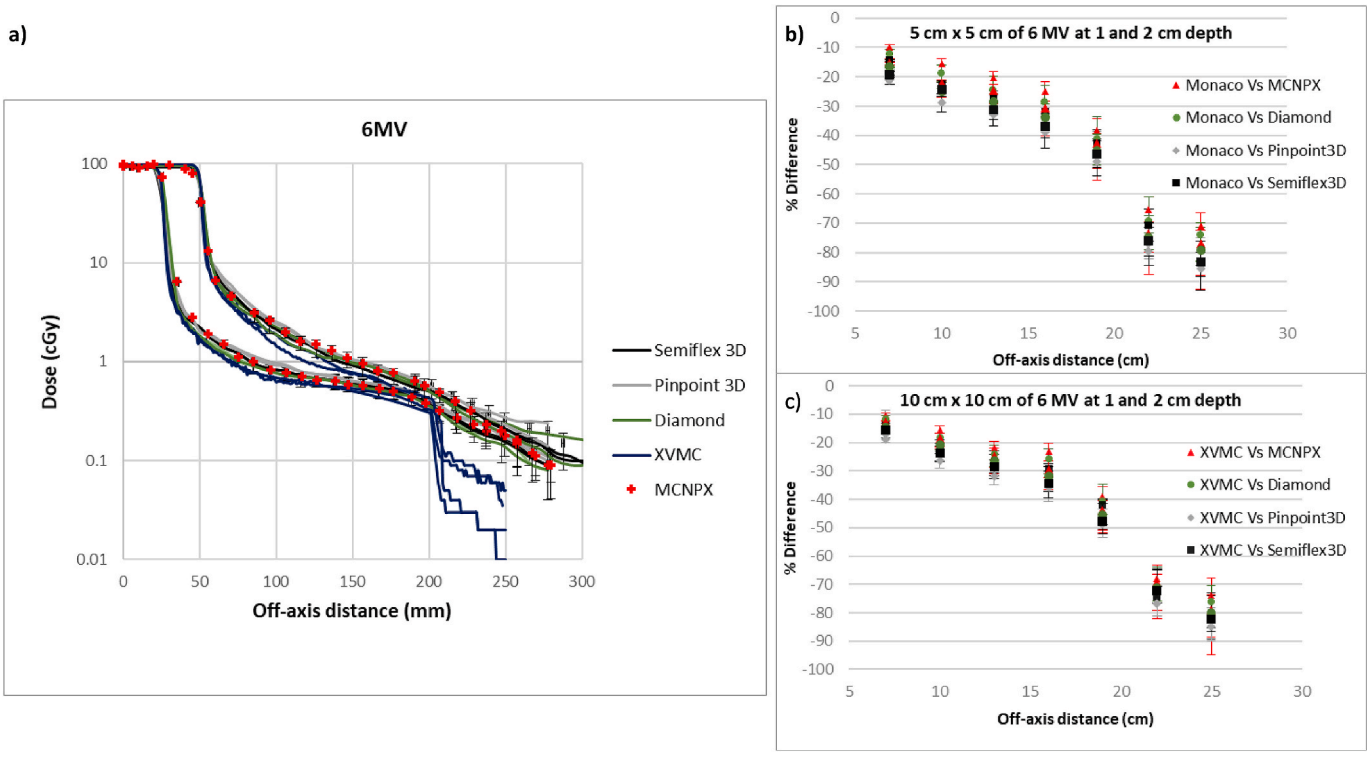

Fig. 4. Comparisons of relative out-of-field photon doses in the cross-plane direction obtained from TPS calculations, MC simulations, and measurements for field sizes of 10 cm x 10 cm and 5 cm x 5 cm of 6 MV at 1 and 2 cm depth (**a**); average of the percentage differences between the results in seven off-axis points for field sizes of 5 cm x 5 cm (**b**) and 10 cm x 10 cm (**c**) at 1 cm and 2 cm depth. The relative uncertainty in the simulated results ranges from 3% near the field edges up to 27.5% in the low-dose region and uncertainty associated with measured data varied between 2 and 13.5%.

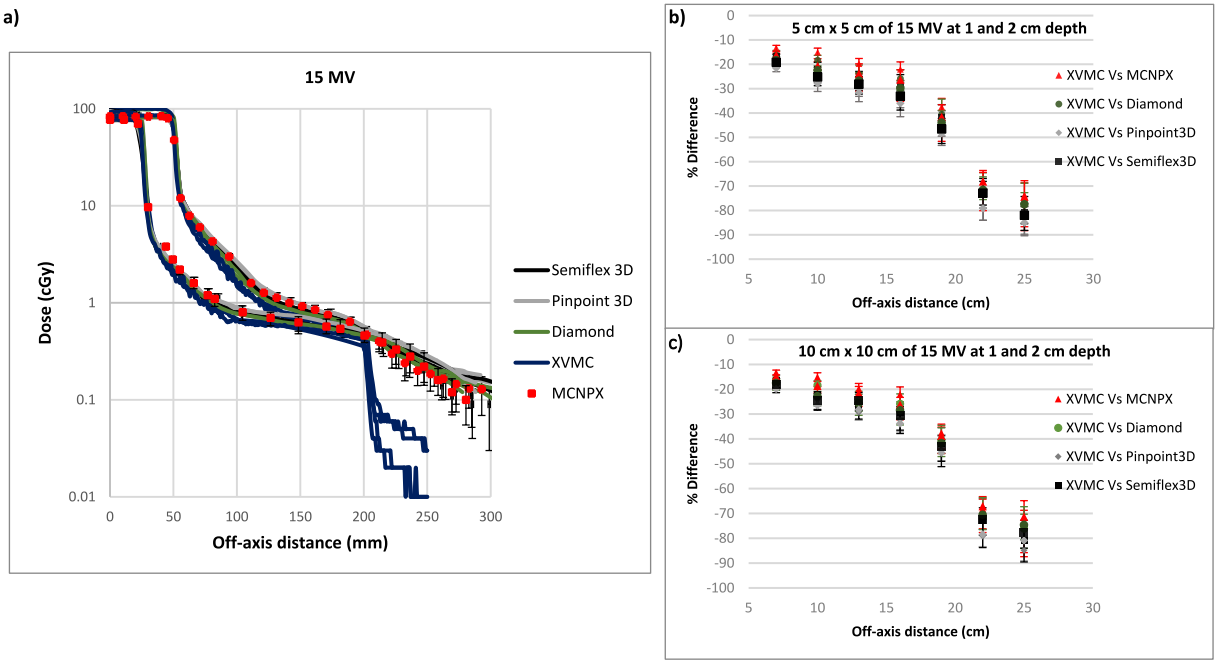

Fig. 5. Comparisons of relative out-of-field photon doses in the cross-plane direction obtained from TPS calculations, MC simulations, and measurements for field sizes of 10 cm x 10 cm and 5 cm x 5 cm of 15 MV at 1 and 2 cm depth (**a**); average of the percentage differences between the results in seven off-axis points for field sizes of 5 cm x 5 cm (**b**) and 10 cm x 10 cm (**c**) at 1 cm and 2 cm depth. The relative uncertainty in the simulated results ranges from 3% near the field edges up to 23% in the low-dose region and uncertainty associated with measured data varied between 2 and 12%.

objective of our study were not aimed at comparing our results with the results reported in (Bednarz and Xu, 2009; Kry et al, 2006, 2007). The first meaningful comparisons that can be made is with out-of-field dose profile data from the 6-MV beam for a field size of 10 cm × 10 cm at a depth of 10 cm and distances less than 30 cm from the isocenter. In this situation, the mean out-of-field dose profile data obtained by our MC

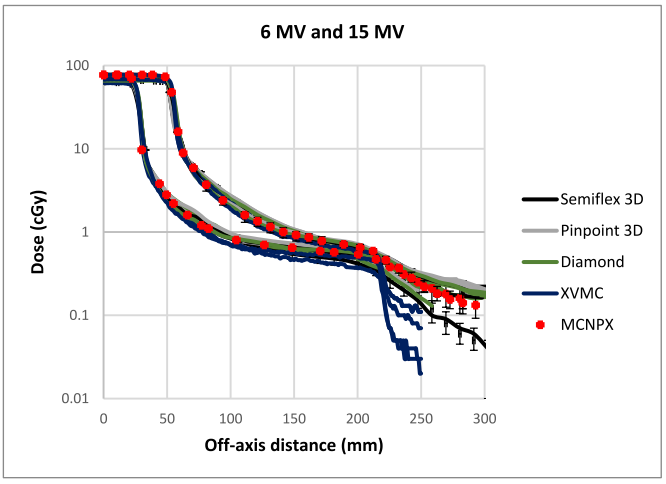

Fig. 6. Comparisons of relative out-of-field photon doses in the cross-plane direction obtained from TPS calculations, MC-simulations, and measurements for field sizes of 10 cm x 10 cm and 5 cm x 5 cm of 6 MV and 15 MV at 10 cm depth. The relative uncertainty in the simulated results ranges from 2% near the field edges up to 18% in the low-dose region.

model was slightly lower (2–5%) compared to values reported by Kry et al. (2006). The second comparison was made between the out-of-field photon dose profiles for 5 cm × 5 cm and 10 cm × 10 cm field at 10 cm and off-axis distance up to 18 cm obtained by our study and those reported by Cravo Sá et al. (Cravo Sá et al., 2020). According to this comparison, the average relative difference between measured and calculated values for both field sizes were again lower (3–7%) in our study. This difference in out-of-field doses is most likely due to differences in the head designs of the Elekta Synergy and the Varian Clinac and 2100 machines (Kry et al., 2017).

Several different studies (Howell et al., 2010; Huang et al., 2013; Wang and Ding, 2014) have assessed the accuracy of out-of-field dose calculations in different TPSs. In a study by Huang et al. (2013), the accuracy of out-of-field dose calculations from the Varian Clinac 2100 by Pinnacle (Direct Machine Parameter Optimization (DMPO) algorithm, Version 9.0) was examined. Shine et al. (2019) investigated the accuracy of out-of-field doses calculated by Eclipse (analytic anisotropic algorithm (AAA), Version 13.7) for the Varian TrueBeam. The comparisons between our results and their results for 6 MV at field sizes of 10 x 10 cm^2 are shown in Table 1. XVMC exhibits less underestimation in the calculation of out-of-field doses but a marked increase in inaccuracy in the out-of-field areas X > 16 cm from the field edge.

Despite the increased accuracy of XVMC found in this study, it should be noted that (as recommended by TG-203) the estimation of the CIED dose by TPS when the CIED is placed beyond 3 cm from the nearest field edge has an unacceptable accuracy (Miften et al., 2019).

In a recent MC study by Sánchez-Nieto et al. (2020), the authors compared out-of-field doses from an Elekta Axesse among collapsed cone convolution (CCC) and XVMC algorithms available in a Monaco TPS, EGSnrc MC code, and measurements only for low energy photon (6 MV). Although these researchers reported both over- and underestimations for the XVMC algorithm, they concluded that XVMC underestimates out-of-field doses in almost all the irradiation scenarios investigated in their study. According to their results, XVMC underestimated out-of-field dose by a maximum of 29% for the 10 × 10 cm^2 field at a depth of 5 cm and up to an off-axis distance of 11.6 cm.

Table 1
Comparison between our results and those reported by Shine et al. (2019) *and* Huang et al. (2013) *for* 6 MV *at field sizes of 10 x 10 cm^2.*

Off-axis distance	Mean underestimation of dose calculation		
	Eclipse (V.13.7, AAA) versus MC (Shine et al., 2019)	Pinnacle (V.9.0, DMPO) versus MC (Huang et al., 2013)	Monaco (V.5.0, XVMC) versus MC (Present study)
X = 7.5 cm	15.4%	18.3%	10.1%
X = 10 cm	16.03%	57.4%	13.2%
X = 14 cm	17.5%	173%	16.7%
X = 16 cm	29.3%	194%	37.3%
X = 22 cm	–	–	64.1%
X = 25 cm	–	–	73.7%

In general, our results for 6 MV showed that the XVMC algorithm underestimated out-of-field doses with average errors of −15.2% (Vs MCNPX) and −18.7% (Vs measurements) at distances less than 10 cm from the field edge and −28.3% (Vs MCNPX) and −33.8% (Vs measurements) at distances of 10 and 16 cm from the field edge. However, the average error was dramatically increased and exceeded −50% for the off-axis points between 16 < X ≤ 25 cm. Based on our results, the inaccuracy of XVMC for out-of-field dose calculation for a 15 MV beam is slightly higher, increasing from 3.5% to 10.7% compared to 6 MV photon.

In addition, the photoneutrons produced at higher energy (≥10 MV) were not considered in the TPS. This is also one limitation of EGSnrc/BEAMnrc code, which is incapable of transporting neutrons, despite its strengths and wide use in medical physics.

The comparison between out-of-field doses at depths of 1, 2 and 10 cm revealed that the influence of depth on out-of-field dose is not large, which is consistent with the results by Kaderka et al. (2012).

There are however some considerations about out-of-field photon dose at CIED depths. CIEDs are typically located 1–2 cm below the patient's skin, which is the main reason for the choice of the model in this study. However, based on CIED type, model and other parameters, it might be implanted at a shallower depth (<1 cm). The first consideration is about uncertainty in the calculations of out-of-field dose at CIED depths. In Figs. 4–6, all error bars, where visible, indicated the uncertainty (one standard deviation) in the simulated and the measured results. The average uncertainty associated with simulated results was up to 28% at CIED depth versus up to 18% at a 10 cm depth. In general, an out-of-field dose at CIED depth was associated with greater statistical uncertainty in the dose estimate. As noted in the figures, uncertainty increases with increasing distance from the central axis and decreasing field size. Fig. 7-b shows the statistical uncertainties in the Monaco results with similar trends ranging between 2% and 21% at the CIED depth and between 1% and 10% at a depth of 10 cm. However, the uncertainty in the measured data was lower than TPS calculations and MC- simulations and ranged from 2% near the field edges up to 14% in the lowest dose region. This difference between uncertainty associated with simulated out-of-field data, TPS calculations, and measured data was also reported by (Delana et al., 2020; Huang et al., 2013; Kry et al, 2006, 2007).

The second consideration involves out-of-field dose measurements at very shallow depths (≅0.5 cm) until a depth of D_{max} due to a build-down effect. Therefore, as noted in AAPM TG-203 (Miften et al., 2019) and recommended by Yan et al. (2018), a 1- to 2-cm bolus should be used depending on CIED depth and irradiation parameters to provide more accurate CIED does calculations and measurements.

3.3. Neutron and CIED relative damage

Validation of our simulated photoneutron spectrum for jaws and MLC closed was conducted using published spectra reported in the literature for the 15 MV Elekta Precise (Abou-Taleb et al., 2018; Howell et al., 2009), and the energy spectra qualitatively were in general agreement.

In Table 2, the highest neutron influence for 10 cm x 10 cm field size at CIED depths obtained from the current study are presented. The neutron fluence increased by increasing depth from 1 cm to 2 cm, reached its maximum value (3.61 *10-10) at D_{max} (2.7 cm), and then

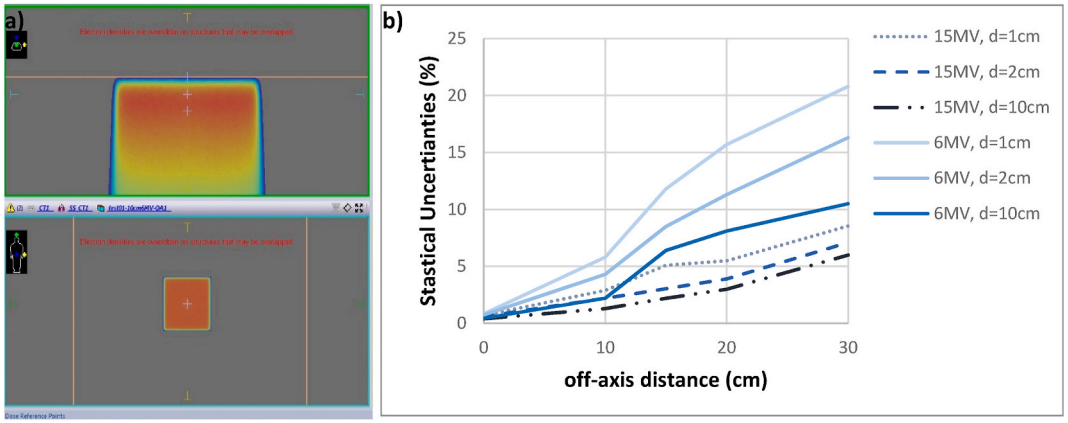

Fig. 7. (**a**) Monaco treatment planning system: Calculated dose distribution on the phantom in sagittal and transverse planes; (**b**) Statistical uncertainties in the Monaco results. An out-of-field photon dose at a shallower CIED depth of 1 cm was associated with greater statistical uncertainty in the dose estimate compared to a CIED depth of 2 cm and clinical depth of 10 cm.

Table 2
The MC calculated neutron fluences per incidence electron at CIED depths for Elekta Synergy (current study) and Precise (previous study) with 15 MV photon energy.

Linac	Neutron fluence Ø(n/cm^2)/e	Depth
Elekta Precise, Abou-Taleb et al. (Abou-Taleb et al., 2018)	$2.17 *10^{-9}$	d = 1 cm
	$2.44*10^{-9}$	d = 2 cm
	$2.47*10^{-9}$	D_{max} = 2.17 cm
Elekta Synergy, **(Present study)**	$3.23 *10^{-10}$	d = 1 cm
	$3.47 *10^{-10}$	d = 2 cm
	$3.61 *10^{-10}$	D_{max} = 2.7

decreased at greater depths. In addition, previously published photoneutron data for 15 MV Elekta Precise medical linac by Abou-Taleb et al. (2018) are presented for comparison.

Comparison between our data and published data (Kaderka et al., 2012; Mesbahi et al., 2010) on neutron dose equivalent as a function of off-axis distance for field size of 5 cm x 5 cm at different depths along the in-plane direction is shown in Fig. 8.

It can be seen from Fig. 8 and Table 2 that total neutron doses and fluences decrease with increasing depth and distance from the field edge. As also stated by Koivunoro et al. (2011), the majority of the total neutron dose at the CIED locations is due to the thermal and epithermal neutrons which usually lead to CIED soft errors.

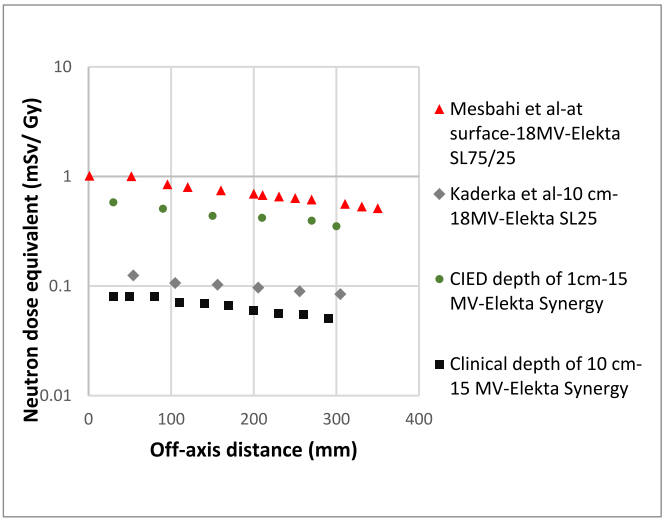

Fig. 8. Neutron dose equivalent as a function of off-axis distance for field size of 5 cm x 5 cm obtained from this study and two published studies.

The CIED relative neutron damage of a 15 MV photon beam from Elekta Synergy as a function of off-axis distance for field size of 10 cm× 10 cm and 5 cm x 5 cm at CIED depths is shown in Fig. 9.

A comparison of our results with those obtained by Ezzati and Studenski (2017) reveals both differences and similarities. Our results showed an average of 36% reduced relative damage at a CIED depth range. This finding is attributed to the fact that higher neutron fluence caused by higher energy photons (18 MV Vs 15 MV) can result in a higher probability of neutron-induced damage. Another equally important reason is that fewer secondary neutron fluences are produced by Elekta compared to Varian, which was investigated in detail by Howell et al. (2009). Similar to the results reported by Ezzati and Studenski (2017), a minimal dependency relationship between field size and CIED relative neutron damage is noted with increasing distance from the field edge. This finding is attributed to the fact that out-of-field neutrons are caused not only by photoneutron production in the linac head but also by neutrons scattered throughout the treatment vault.

Matsubara et al. (2020) quantitatively investigated the neutron contribution to CIED malfunction, suggesting that the risk of a CIED can be expressed by a linear relationship to neutron dose. However, given the stochastic nature of neutron-induced events, TG 203 highly recommends avoiding using neutron-producing therapy (15 and 18 MV photon or proton therapy) to treat CIED patients with cancer.

4. Conclusion

In this study, the accuracy of out-of-field dose calculations using the XVMC Monte Carlo dose engine in the Monaco TPS was investigated for both low- (6 MV) and high-energy (15 MV) photons at CIED depths based on a comparison between MCNPX simulated out-of-field doses and measured out-of-field doses using three high spatial and sensitive active detectors.

Out-of-field photon doses were analyzed in both in-plane and cross-plane directions. The overall average results showed that for 6-MV photons, the XVMC algorithm underestimated out-of-field doses with average errors of −17% at distances less than 10 cm from the field edge and −31% at distances between $10 < X \leq 16$ cm from the field edge. The average error was dramatically increased and exceeded −50% for the off-axis points between $16 < X \leq 25$ cm. However, the inaccuracy of XVMC for out-of-field dose calculation from high-energy photons (15 MV) was higher, increasing from 3.5% to 10.7% compared to 6-MV photons. According to the results, an out-of-field dose at a shallower CIED depth was associated with greater statistical uncertainty in the

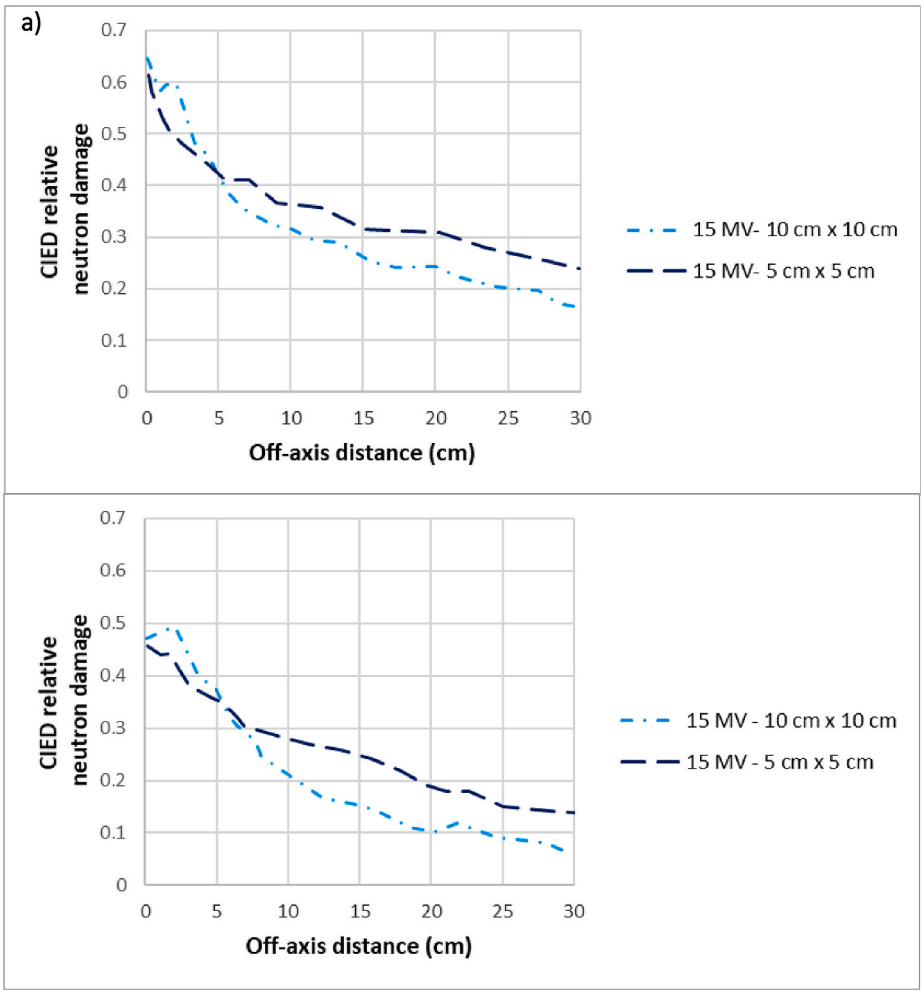

Fig. 9. CIED relative neutron damage of a 15 MV photon beam from Elekta Synergy at 1 cm (**a**) and 2 cm (**b**) depth as a function of field size and off-axis distance.

dose estimate (up to 21% at a 1 cm depth versus up to 10.5% at 10 cm). Therefore, uncertainty in out-of-field dose calculations at CIED depths should be considered.

In addition, this study conducted a photon out-of-field dose analysis of three clinically available detectors. Although all three studied detectors could be used for an accurate out-of-field dose measurement, the results showed that Diamond almost always measured the lowest but provided a closer reading to the MC-simulated out-of-field dose, thus demonstrating the most reliable measurements.

Finally, neutron equivalent dose and fluence at CIED depths of 15 MV Elekta Synergy were estimated using MCNPX at CIED depths (1 and 2 cm) up to an off-axis distance of 30 cm, and corresponding CIED relative neutron damage was quantified. Our results showed that the relative neutron damage at a CIED depth range for 15 MV photon is 36% less than that reported for 18 MV photon in the literature.

Author statement

Hossein Aslian: Conceptualization, Methodology, Software, Formal analysis, Writing - original draft, Visualization. Mara Severgnini: Methodology, Formal analysis, Supervision. Navid Khaledi: Software, Validation, Data curation, Visualization. Stefano Ren Kaiser: Validation, Visualization. Anna Delana: Validation, Visualization. Rossella Vidimari: Formal analysis. Mario de Denaro: Resources, Project administration. Francesco Longo. Methodology, Data curation, Supervision.

Declaration of competing interest

The authors declare that they have no known competing financial interests or personal relationships that could have appeared to influence the work reported in this paper.

Acknowledgment

We would like to acknowledge Elekta for providing us with the detailed information on the Elekta Synergy linear accelerator.

References

Abdelaal, A.M., Attalla, E.M., Elshemey, W.M., 2017. Dose estimation outside radiation field using Pinpoint and Semiflex ionization chamber detectors. Radiat. Phys. Chem. 139, 120–125. https://doi.org/10.1016/j.radphyschem.2017.04.006.

Abou-Taleb, W.M., Hassan, M.H., El Mallah, E.A., Kotb, S.M., 2018. MCNP5 evaluation of photoneutron production from the Alexandria University 15 MV Elekta Precise medical LINAC. Appl. Radiat. Isot. 135, 184–191. https://doi.org/10.1016/j.apradiso.2018.01.036.

Aslian, H., Delana, A., Kaiser, S.R., Moretti, E., Foti, C., Bregant, P., de Denaro, M., Longo, F., Severgnini, M., 2018. A multicenter dosimetry study to evaluate the imaging dose from Elekta XVI and Varian OBI kV-CBCT systems to cardiovascular implantable electronic devices (CIEDs). Phys. Med. 55, 40–46. https://doi.org/10.1016/j.ejmp.2018.10.013.

Aslian, H., Kron, T., Longo, F., Rad, R., Severgnini, M., 2019. A review and analysis of stereotactic body radiotherapy and radiosurgery of patients with cardiac implantable electronic devices. Australas. Phys. Eng. Sci. Med. https://doi.org/10.1007/s13246-019-00751-8.

Aslian, H., Kron, T., Watts, T., Akalanli, C., Hardcastle, N., Lonski, P., Montaseri, A., Hay, B., Korte, J., Berk, K., Longo, F., Severgnini, M., 2020. The effect of stereotactic body radiotherapy (SBRT) using flattening filter-free beams on cardiac implantable

electronic devices (CIEDs) in clinical situations. J. Appl. Clin. Med. Phys. 21, 121–131. https://doi.org/10.1002/acm2.12873.
Becker, J., 2007. Simulation of Neutron Production at a Medical Linear Accelerator. Department of Radiotherapy and Radio-Oncology, Medical Physics: Department of Physics, University of Hamburg performed at the University Medical Center Hamburg-Eppendorf.
Bednarz, B., Xu, X.G., 2009. Monte Carlo modeling of a 6 and 18 MV Varian Clinac medical accelerator for in-field and out-of-field dose calculations: development and validation. Phys. Med. Biol. 54 https://doi.org/10.1088/0031-9155/54/4/N01.
Clements, M., Schupp, N., Tattersall, M., Brown, A., Larson, R., 2018. Monaco treatment planning system tools and optimization processes. Med. Dosim. https://doi.org/10.1016/j.meddos.2018.02.005.
Cravo Sá, A., Barateiro, A., Bednarz, B., Borges, C., Pereira, J., Baptista, M., Pereira, M., Zarza-Moreno, M., Almeida, P., Vaz, P., Madaleno, T., Romanets, Y., 2020. Assessment of out-of-field doses in radiotherapy treatments of paediatric patients using Monte Carlo methods and measurements. Phys. Med. 71, 53–61. https://doi.org/10.1016/j.ejmp.2020.02.008.
Delana, A., Barbareschi, A., Consorti, R., Falco, M.D., 2020. Dose calculation accuracy in proximity of a pacemaker: a multicenter study with three commercial treatment planning systems. Phys. Med.: Eur. J. Med. Plants 80, 201–208. https://doi.org/10.1016/J.EJMP.2020.10.015.
DePriest, K.R., 2014. Impact of ASTM Standard E722 Update on Radiation Damage Metrics. https://doi.org/10.2172/1177052. Albuquerque, NM, and Livermore, CA (United States).
Ezzati, A.O., Studenski, M.T., 2019. Design of a neutron applicator to reduce damage in cardiac implantable electronic devices. Eur. Phys. J. Plus 134, 1–6. https://doi.org/10.1140/epjp/i2019-12851-3.
Ezzati, A.O., Studenski, M.T., 2017. Neutron damage induced in cardiovascular implantable electronic devices from a clinical 18 MV photon beam: a Monte Carlo study. Med. Phys. 44, 5660–5666. https://doi.org/10.1002/mp.12581.
Gauter-Fleckenstein, B., Barthel, C., Büttner, S., Wenz, F., Borggrefe, M., Tülümen, E., 2020. Effectivity and applicability of the German DEGRO/DGK-guideline for radiotherapy in CIED-bearing patients. Radiother. Oncol. 152, 208–215. https://doi.org/10.1016/j.radonc.2020.01.006.
Gholampourkashi, S., Cygler, J.E., Belec, J., Vujicic, M., Heath, E., 2019. Monte Carlo and analytic modeling of an Elekta Infinity linac with Agility MLC: investigating the significance of accurate model parameters for small radiation fields. J. Appl. Clin. Med. Phys. 20, 55–67. https://doi.org/10.1002/acm2.12485.
Howell, R.M., Kry, S.F., Burgett, E., Hertel, N.E., Followill, D.S., 2009. Secondary neutron spectra from modern Varian, Siemens, and Elekta linacs with multileaf collimators. Med. Phys. 36, 4027–4038. https://doi.org/10.1118/1.3159300.
Howell, R.M., Scarboro, S.B., Kry, S.F., Yaldo, D.Z., 2010. Accuracy of out-of-field dose calculations by a commercial treatment planning system. Phys. Med. Biol. 55, 6999–7008. https://doi.org/10.1088/0031-9155/55/23/S03.
Huang, J.Y., Followill, D.S., Wang, X.A., Kry, S.F., 2013. Accuracy and sources of error of out-of field dose calculations by a commercial treatment planning system for inte sity-modulated radiation therapy treatments. J. Appl. Clin. Med. Phys. 14, 186–197. https://doi.org/10.1120/jacmp.v14i2.4139.
ICRP, 1996. Conversion coefficients for use in radiological protection against external radiation, ICRP publication 74. Ann. ICRP 26 (3–4).
Implementation of the International Code of Practice on Dosimetry in Radiotherapy TRS 398: Review of Testing Results | IAEA [WWW Document], n.d. URL https://www.iaea.org/publications/8456/implementation-of-the-international-code-of-practice-on-dosimetry-in-radiotherapy-trs-398-review-of-testing-results (accessed 11.11.20).
Kaderka, R., Schardt, D., Durante, M., Berger, T., Ramm, U., Licher, J., Tessa, C. La, 2012. Out-of-field dose measurements in a water phantom using different radiotherapy modalities. Phys. Med. Biol. 57, 5059–5074. https://doi.org/10.1088/0031-9155/57/16/5059.
Khaledi, N., Aghamiri, M., Aslian, H., Ameri, A., 2017. Tabulated square-shaped source model for linear accelerator electron beam simulation. J. Canc. Res. Therapeut. 13, 69–79. https://doi.org/10.4103/0973-1482.206235.
Khaledi, N., Arbabi, A., Sardari, D., Rabie Mahdavi, S., Aslian, H., Dabaghi, M., Sheibani, K., 2013. Monte Carlo investigation of the effect of small cutouts on beam profile parameters of 12 and 14 MeV electron beams. Radiat. Meas. 51–52, 48–54. https://doi.org/10.1016/j.radmeas.2013.01.019.
Khaledi, N., Dabaghi, M., Sardari, D., Samiei, F., Ahmadabad, F.G., Jahanfarnia, G., Saadi, M.K., Wang, X., 2018. Investigation of photoneutron production by Siemens artiste linac: a Monte Carlo Study. Radiat. Phys. Chem. 153, 98–103. https://doi.org/10.1016/j.radphyschem.2018.06.006.
Koivunoro, H., Serén, T., Hyvönen, H., Kotiluoto, P., Iivonen, P., Auterinen, I., Seppälä, T., Kankaanranta, L., Pakarinen, S., Tenhunen, M., Savolainen, S., 2011. Epithermal neutron beam interference with cardiac pacemakers. Appl. Radiat. Isot. 69, 1904–1906. https://doi.org/10.1016/j.apradiso.2011.03.028.
Kry, S.F., Bednarz, B., Howell, R.M., Dauer, L., Followill, D., Klein, E., Paganetti, H., Wang, B., Wuu, C.S., George Xu, X., 2017. AAPM TG 158: measurement and calculation of doses outside the treated volume from external-beam radiation therapy. Med. Phys. 44, e391–e429. https://doi.org/10.1002/mp.12462.
Kry, S.F., Titt, U., Followill, D., Pönisch, F., Vassiliev, O.N., White, R.A., Stovall, M., Salehpour, M., 2007. A Monte Carlo model for out-of-field dose calculation from high-energy photon therapy. Med. Phys. 34, 3489–3499. https://doi.org/10.1118/1.2756940.
Kry, S.F., Titt, U., Pönisch, F., Followill, D., Vassiliev, O.N., Allen White, R., Mohan, R., Salehpour, M., 2006. A Monte Carlo model for calculating out-of-field dose from a Varian 6 MV beam. Med. Phys. 33, 4405–4413. https://doi.org/10.1118/1.2360013.
Martens, C., De Wagter, C., De Neve, W., 2000. The value of the PinPoint ion chamber for characterization of small field segments used in intensity-modulated radiotherapy. Phys. Med. Biol. 45, 2519–2530. https://doi.org/10.1088/0031-9155/45/9/306.
Martnez Ovalle, S.A., 2013. Neutron dose equivalent in tissue due to linacs of clinical use. In: Frontiers in Radiation Oncology. InTech. https://doi.org/10.5772/56513.
Matsubara, H., Ezura, T., Hashimoto, Y., Karasawa, K., Nishio, T., Tsuneda, M., 2020. Prediction of radiation-induced malfunction for cardiac implantable electronic devices (CIEDs). Med. Phys. 47, 1489–1498. https://doi.org/10.1002/mp.14057.
Mesbahi, A., 2006. Development a simple point source model for Elekta SL-25 linear accelerator using MCNP4C Monte Carlo code. J. Radiat. Res. Int. J. Radiat. Res.
Mesbahi, A., Keshtkar, A., Mohammadi, E., Mohammadzadeh, M., 2010. Effect of wedge filter and field size on photoneutron dose equivalent for an 18 MV photon beam of a medical linear accelerator. Appl. Radiat. Isot. 68, 84–89. https://doi.org/10.1016/j.apradiso.2009.08.008.
Miften, M., Mihailidis, D., Kry, S.F., Reft, C., Esquivel, C., Farr, J., Followill, D., Hurkmans, C., Liu, A., Gayou, O., Gossman, M., Mahesh, M., Popple, R., Prisciandaro, J., Wilkinson, J., 2019. Management of radiotherapy patients with implanted cardiac pacemakers and defibrillators: a Report of the AAPM TG-203†. Med. Phys. 46, e757–e788. https://doi.org/10.1002/mp.13838.
Muraro, S., Battistoni, G., Kraan, A.C., 2020. Challenges in Monte Carlo simulations as clinical and research tool in particle therapy: a review. Front. Phys. https://doi.org/10.3389/fphy.2020.567800.
Pelowitz, D.B., Durkee, J.W., Elson, J.S., Fensin, M.L., James, M.R., Johns, R.C., McKinney, G.W., Mashnik, S.G., Waters, L.S., Wilcox, T.A., 2011. MCNPX User's Manual. Version 2.7.0. Los Alamos National Laboratory report LA-CP-11-00438.
Puchalska, M., Sihver, L., 2015. PHITS simulations of absorbed dose out-of-field and neutron energy spectra for ELEKTA SL25 medical linear accelerator. Phys. Med. Biol. 60, N261–N270. https://doi.org/10.1088/0031-9155/60/12/N261.
Richmond, N., Allen, V., Wyatt, J., Codling, R., 2020. Evaluation of the RayStation electron Monte Carlo dose calculation algorithm. Med. Dosim. 45, 159–167. https://doi.org/10.1016/j.meddos.2019.09.003.
Sánchez-Nieto, B., Medina-Ascanio, K.N., Rodríguez-Mongua, J.L., Doerner, E., Espinoza, I., 2020. Study of out-of-field dose in photon radiotherapy: a commercial treatment planning system versus measurements and Monte Carlo simulations. Med. Phys. 47, 4616–4625. https://doi.org/10.1002/mp.14356.
Shine, N.S., Paramu, R., Gopinath, M., Jaon Bos, R.C., Jayadevan, P.M., 2019. Out-of-field dose calculation by a commercial treatment planning system and comparison by Monte Carlo simulation for varian TrueBeam®. J. Med. Phys. 44, 156–175. https://doi.org/10.4103/jmp.JMP_82_18.
Sikora, M., Dohm, O., Alber, M., 2007. A virtual photon source model of an Elekta linear accelerator with integrated mini MLC for Monte Carlo based IMRT dose calculation. Phys. Med. Biol. 52, 4449–4463. https://doi.org/10.1088/0031-9155/52/15/006.
Snyder, J.E., Hyer, D.E., Flynn, R.T., Boczkowski, A., Wang, D., 2019. The commissioning and validation of Monaco treatment planning system on an Elekta VersaHD linear accelerator. J. Appl. Clin. Med. Phys. 20, 184–193. https://doi.org/10.1002/acm2.12507.
Venselaar, J., Welleweerd, H., Mijnheer, B., 2001. Tolerances for the accuracy of photon beam dose calculations of treatment planning systems. Radiother. Oncol. 60, 191–201. https://doi.org/10.1016/S0167-8140(01)00377-2.
Wang, L., Ding, G.X., 2014. The accuracy of the out-of-field dose calculations using a model based algorithm in a commercial treatment planning system. Phys. Med. Biol. 59 https://doi.org/10.1088/0031-9155/59/13/N113.
Yan, H., Guo, F., Zhu, D., Stryker, S., Trumpore, S., Roberts, K., Higgins, S., Nath, R., Chen, Z., Liu, W., 2018. On the use of bolus for pacemaker dose measurement and reduction in radiation therapy. J. Appl. Clin. Med. Phys. 19, 125–131. https://doi.org/10.1002/acm2.12229.